

generated methanol and a stirbar inside a nitrogen glovebag. A 0.13-mL aliquot of the solution of **4** was diluted to 3.0 mL and the solution was removed from the glovebag. The diluted solution contained 18 nmol of **4** per g of solution. Inside the nitrogen glovebag a 0.26-mL aliquot of **4** was added to a cuvette and diluted to 3.0 mL. The cuvette was then sealed with a septum. To 27.7 mg of 80% pure sodium dithionite (1.27×10^{-4} mol) in a 10-mL volumetric flask was added deoxygenated water inside the nitrogen glovebag. With use of a 100- μ L syringe, 15 μ L of the sodium dithionite solution was injected into the cuvette containing **4** producing **9** with a concentration of 35 nmol/g of solution. Fluorescence spectra of the solutions of **1**, **3**, **4**, and **9** were then measured with

excitation and emission slits set at 8 nm. The results are summarized in Table I.

Acknowledgment. This investigation was supported by PHS Grant CA-24665, DHHS and BRS Grant RR07013 (1986) awarded by the Biomedical Research Support Grant Program, Division of Research Resources, NIH. The authors also thank Drs. Sergio Penco and Federico Arcamone of Farmitalia Carlo Erba for a generous sample of daunomycin and Dr. Steven Avrebuch of NCI for a generous sample of 5-iminodaunomycin.

Conformational Analysis of Lipophilic Antifolates: Crystal and Molecular Structures of 6-Substituted 5-Adamantyl-2,4-diaminopyrimidines by X-ray Analysis and Molecular Mechanics Calculations

Vivian Cody,* Paul A. Sutton, and William J. Welsh†

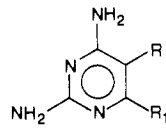
Contribution from the Medical Foundation of Buffalo, Buffalo, New York 14203, and the University of Cincinnati, Cincinnati, Ohio 45221. Received November 21, 1986

Abstract: The results of crystal structure determinations and molecular mechanics force field calculations on a series of four 6-substituted 5-adamantyl-2,4-diaminopyrimidine antifolates show that the pyrimidine ring and its substituents become more distorted from planarity as the size of the 6-substituent increases. These distortions are caused by the steric interference of the adamantyl hydrogen atoms with those of the 4,6-pyrimidine ring substituents. This series of antifolates shows a 500-fold increase in their cytotoxic activity against mammalian dihydrofolate reductase when the 6-substituent is increased from hydrogen to methyl to ethyl but drops at propyl. Full relaxation MM2P conformational energy profiles for rotation about the pyrimidine-adamantyl bond show that the maximum energy barrier (~ 6 kcal/mol) is located at 60° within the 0 – 120° unique conformational space studied. The structurally observed conformations of the 6-H and 6-methyl analogues are located at energy minima, whereas the most active antifolate 6-ethyl and 6-propyl analogues are observed in high energy conformations. The crystal structure of the 6-ethyl antifolate also reveals a (67/33% occupancy) disorder in the methylene carbon of the ethyl side chain which makes several short intramolecular H \cdots H contacts with the adamantyl hydrogen atoms. This conformation may be stabilized in the crystal by intermolecular interactions not considered in the present force field calculations. Such stabilization could also be operative at the enzyme binding site and thus contribute to the 6-ethyl analogue's high potency.

Lipophilic diaminopyrimidines are a class of drugs that act as inhibitors of dihydrofolate reductase (DHFR) and have been developed for use as antimalarial, antibiotic, or anticancer agents. These drugs also show striking differences in their inhibitory activity with only small changes in their chemical structures.¹⁻³ It has been demonstrated that the principal structural characteristic necessary for binding to dihydrofolate reductase of any species is a 2,4-diaminopyrimidine, *s*-triazine, or pteridine ring structure.⁴ Structure-activity studies of 2,4-diaminopyrimidines further indicate that a lipophilic group at position five is also essential for tight binding to DHFR.⁵ Large differences in inhibitory potency have been observed concomitant with small changes in the chemical structures of these antifolate drugs.

Comparison of several lipophilic antifolates shows that those with a 5-adamantyl substituent are the most effective inhibitors of mammalian DHFR with potencies greater than the chemotherapeutic agent methotrexate (MTX).⁵⁻⁸ As illustrated (Table I), these structures have greater binding affinities for DHFR than those antifolates with comparable molar volumes and hydrophobicities.^{7,8} Additionally, there is a sharp increase in cytotoxic activity of 5-adamantyl 6-substituted antifolates within the series with 6-H < propyl < methyl < ethyl (Table I). These adamantyl antifolates also have cellular uptake rates about 10 000 times more rapid than MTX and show strong cytotoxic activity in culture cells.^{9,10}

Table I. Structure-Activity Relationships among Lipophilic Diaminopyrimidine Inhibitors of DHFR



R	R ₁	X-ray structure	ID ₅₀ , ^a μ M
adamantyl	hydrogen	DAHMP	3.3×10^{-7}
adamantyl	methyl	DAMP	6.0×10^{-9}
adamantyl	ethyl	DAEP	2.5×10^{-10}
adamantyl	propyl	DAPP	4.8×10^{-8}
cyclohexyl	methyl	DCXMP	3.9×10^{-7}
hexyl	methyl	DHXMP	1.2×10^{-6}
heptyl	methyl	DHMP	1.6×10^{-6}
<i>tert</i> -butyl	methyl	DTMP	1.9×10^{-5}
1-naphthyl	methyl	DNMP-1	5.6×10^{-4}
2-naphthyl	methyl	DNMP-2	7.0×10^{-8}
methotrexate		MTX	8.0×10^{-9}

^a 50% growth inhibition of mouse mammary adenocarcinoma cells (TA3) in culture.⁷

In order to investigate the structural, conformational, and electronic properties of this series of 5-adamantyl lipophilic an-

* Send reprint requests to: Dr. Vivian Cody, Medical Foundation of Buffalo, Inc., 73 High St., Buffalo, New York 14203.

† University of Cincinnati. Current address: Department of Chemistry, University of Missouri-St. Louis, St. Louis, MO, 63121.

(1) Hitchings, G. H.; Burchall, J. J. *Adv. Enzymol.* **1965**, *27*, 417-468.
(2) Blakley, R. L.; Benkovic, S. J. *Folates and Pterines*; Wiley: New York, 1984; Vol. 1.
(3) Roth, B.; Cheng, C. C. *Prog. Med. Chem.* **1982**, *19*, 270-331.

Table II. 5-Adamantyl 6-Substituted Diaminopyrimidine Conformations^a

torsion angle	DAHP	DAMP1	DAMP2	DAEP	DAPP
C(6)-C(5)-C(7)-C(8)	-3	-13	-8	55	147
C(6)-C(5)-C(7)-C(14)	116	-131	-125	-66	-91
C(6)-C(5)-C(7)-C(15)	-121	107	112	173	32
C(7)-C(5)-C(6)-C(61) ^b		-10	-12	20	16
C(5)-C(6)-C(61)-C(62) ^b				-165/161	-111
C(6)-C(61)-C(62)-C(63)					-168

^aAll values are in degrees. ^bAtom C(61) is disordered (67/33% occupancy) in this structure.

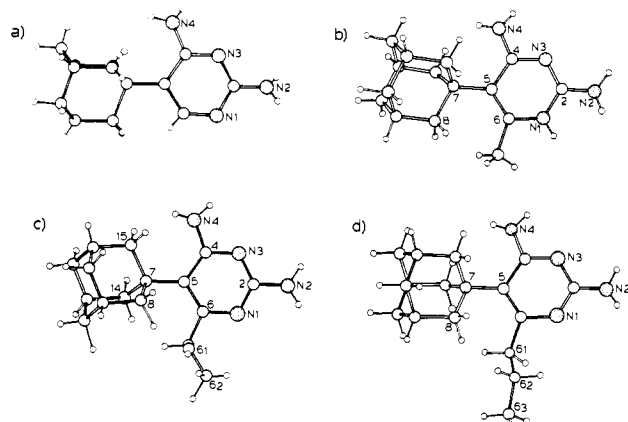


Figure 1. Molecular conformation of 6-substituted 2,4-diamino-5-(1-adamantyl)pyrimidines: (a) 6-hydrogen (DAHP), (b) 6-methyl (DAMP1), (c) 6-ethyl (DAEP), and (d) 6-propyl (DAPP).

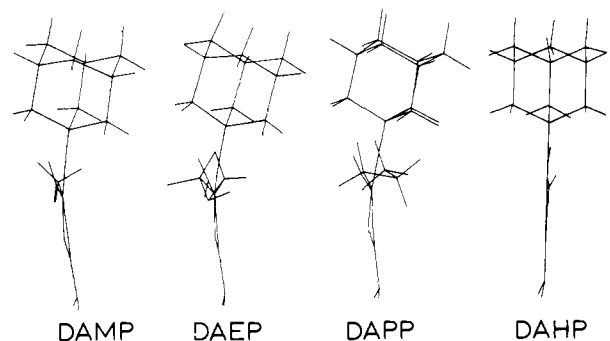


Figure 2. Comparison of the bowed shape of DAMP, DAEP, and DAPP with a planar DAHP.

tifolates, X-ray crystallographic analysis in conjunction with both molecular orbital (MO) and molecular mechanics (MM) calculations was carried out and is reported here.

Results and Discussion

Crystal and Molecular Structure Analysis. The crystallographically observed molecular conformations of 2,4-diamino-5-(1-adamantyl)-6-hydrogen (DAHP), 6-methyl (DAMP1, DAMP2),¹¹ 6-ethyl (DAEP), and 6-propyl (DAPP) pyrimidine are illustrated in Figure 1. Because of the equivalent environment of the adamantyl ring, rotation about the pyrimidine-adamantyl bond (C(5)-C(7)) results in conformationally equivalent rotamers every 120°. As demonstrated (Table II), several adamantyl rotamers have been observed.

These studies reveal that within this series the pyrimidine ring in each structure but DAHP is distorted from planarity with

- (4) Burchall, J. J.; Hitchings, G. H. *Mol. Pharmacol.* **1965**, *1*, 126-136.
 (5) Zakrzewski, S. F. *J. Biol. Chem.* **1963**, *238*, 1485-1490, 4002-4004.
 (6) Jonak, J. P.; Zakrzewski, S. F.; Mead, L. H. *J. Med. Chem.* **1971**, *14*, 408-411; **1972**, *15*, 662-665.
 (7) Kavai, I.; Mead, L. H.; Drobnik, J.; Zakrzewski, S. F. *J. Med. Chem.* **1975**, *18*, 272-275.
 (8) Zakrzewski, S. F.; Dave, C.; Rosen, F. *JNCI, J. Natl. Cancer Inst.* **1978**, *60*, 1029-1033.
 (9) Greco, W. R.; Hakala, M. T. *Mol. Pharmacol.* **1980**, *18*, 521-528.
 (10) Greco, W. R.; Hakala, M. T. *Pharmacol. Exp. Ther.* **1980**, *212*, 39-46.
 (11) Cody, V.; Zakrzewski, S. F. *J. Med. Chem.* **1982**, *25*, 427-431.

Table III. Deviations (Å) of Atoms N(2), N(4), C(7), C(61), C(2), and C(5) from the Least-Squares Plane Through N(1), N(3), C(4), and C(6)

structure	N(2)	N(4)	C(7)	C(61)	C(2)	C(5)
DAHP	0.015	-0.040	0.036	0.031	0.004	0.024
DAMP1	-0.149	0.291	-0.415	-0.047	-0.060	-0.135
DAMP2	-0.233	0.238	-0.419	0.055	-0.088	-0.121
DAEPA ^a	-0.254	0.241	-0.461	0.418	-0.087	-0.122
DAEPB	-0.254	0.241	-0.461	-0.405	-0.087	-0.122
DAPP	-0.291	0.372	-0.470	0.180	-0.132	-0.160

^aAtom C(61) is disordered (67/33% occupancy) in this structure.

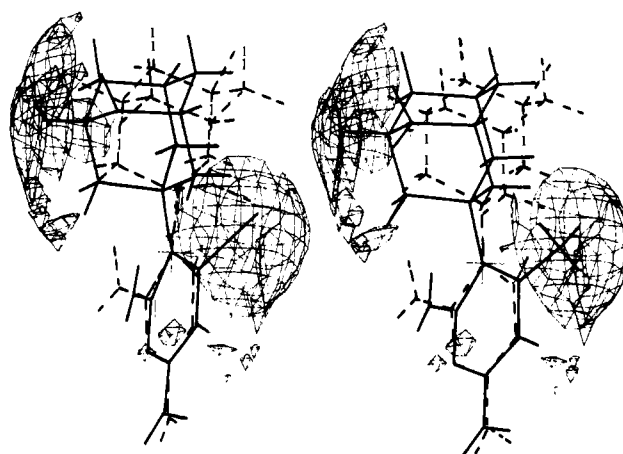


Figure 3. Stereo diagram showing the van der Waals surface remaining when the planar DAHP is subtracted from that of DAMP2.

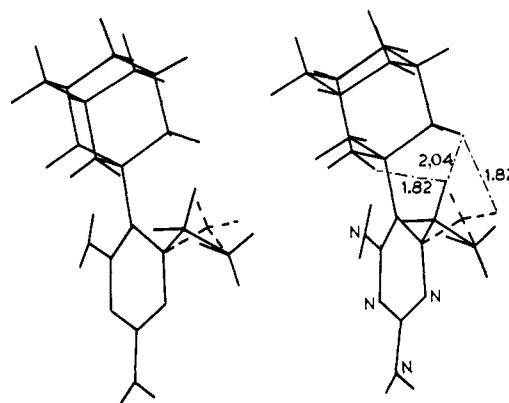


Figure 4. Stereo diagram of DAEP showing the two disordered positions for atom C(61) of the ethyl side chain. Also shown are the close intramolecular H...H contacts made between H(61), H(8A), and H(14) of the adamantyl ring.

respect to its substituents. Placement of the bulky, structurally rigid, adamantyl group adjacent to the 4-amino and 6-alkyl substituents produces unfavorable nonbonded interactions among the adamantyl hydrogen atoms and those of the 4,6-substituents such that there are intramolecular nonbonded H...H contacts less than 2.0 Å in each structure. As a consequence of this steric crowding, the pyrimidine ring becomes increasingly distorted from planarity as the size of the 6-substituent increases. This causes a significant displacement of the pyrimidine ring substituents from the best plane through N(1), N(3), C(4), and C(6) (Table III).

Table IV. Pyrimidine Ring Geometry from Crystallographic Data

	DAHP	DAMP1 ⁺	DAMP2 ⁺	DAEP	DAPP ⁺
Bond Lengths, Å					
esd	(4)	(3)	(3)	(4)	(8)
N(1)-C(2)	1.343	1.341	1.376	1.349	1.370
C(2)-N(3)	1.343	1.324	1.345	1.331	1.364
N(3)-C(4)	1.343	1.346	1.322	1.323	1.341
C(4)-C(5)	1.340	1.463	1.353	1.336	1.315
C(5)-C(6)	1.434	1.379	1.460	1.453	1.482
C(6)-N(1)	1.382	1.365	1.373	1.408	1.368
C(2)-N(2)	1.334	1.315	1.328	1.353	1.296
C(4)-N(4)	1.344	1.337	1.332	1.365	1.346
C(5)-C(7)	1.532	1.547	1.551	1.554	1.547
C(6)-C(61)		1.510	1.511	1.527	1.512
Bond Angles, deg					
esd	(2)	(2)	(2)	(2)	(4)
N(1)-C(2)-N(3)	125.5	120.8	120.7	125.0	118.0
C(2)-N(3)-C(4)	118.2	117.2	118.1	117.3	119.2
N(3)-C(4)-C(5)	122.1	124.3	123.5	123.5	124.2
C(4)-C(5)-C(6)	112.5	112.7	113.5	111.8	111.5
C(5)-C(6)-N(1)	127.4	119.6	119.9	123.8	120.9
C(6)-N(1)-C(2)	114.3	123.4	122.5	116.9	122.4
N(1)-C(2)-N(2)	117.6	117.7	117.8	117.2	119.3
N(3)-C(2)-N(2)	116.9	121.4	121.5	117.8	122.5
N(3)-C(4)-N(4)	114.3	112.2	113.0	112.0	112.8
C(5)-C(4)-N(4)	123.7	123.5	123.5	124.5	122.8
C(4)-C(5)-C(7)	124.7	121.4	120.3	125.9	122.6
C(6)-C(5)-C(7)	122.7	125.9	126.2	122.1	125.9
C(5)-C(6)-C(61)		130.4	130.2	123.6	128.7
N(1)-C(6)-C(61)		110.0	109.9	110.8	110.0

The pyrimidine ring becomes a flattened boat with C(2) and C(5) above the plane. As a result, these antifolates adopt a "bowed" shape (Figure 3). These distortions are further illustrated (Figure 4) by the residual van der Waals surface remaining when the structure of the planar DAHP is subtracted from that of DAMP1.

Analysis of DAEP reveals a positional disorder (67/33% occupancy) of the ethyl side-chain atom C(61). As shown (Figure 4), H(61) is common to both C(61) positions and makes close intramolecular H...H contacts with H(8B) and H(14) of the adamantyl ring, whereas H(61B) makes close contacts only to H(14). There are four other molecular conformations of DAEP observed in a disordered hydrate crystal structure with two molecules in the asymmetric unit.¹² The adamantyl ring in both molecules is rotationally disordered (67/33% occupancy). The conformation of one disordered model is a high energy form and the other is an energy minimum. However, the poor resolution of these data ($R = 18\%$) preclude further analysis.

Although there are only five crystal structures for comparison, two free bases (DAHP and DAEP) and three protonated at N(1), analysis of the pyrimidine ring bonding geometry provides information concerning the tautomeric and mesomeric structures accessible to this ring. As shown (Table IV), there is considerable variation observed in the bond lengths of these five structures. The average of the four endocyclic C-N bonds is 1.353 (5) Å, while that of the two exocyclic C-N bonds is 1.338 (5) Å, suggesting pronounced double bond character in the amino groups. Furthermore, there is less variation in the average bond lengths involving N(3) than N(1). Comparison of the bonds at C(2) indicates that N(1) protonation causes the N(1)-C(2) bond to lengthen and the C(2)-N(2) bond to shorten, while there is little effect on the C(2)-N(3) bond length. This pattern is consistent with similar values reported for other 2,4-diaminopyrimidine antifolates.^{13,14} These distortions cause a shift in the electronic charge density within the ring, thereby decreasing its aromatic character.

(12) Cody, V.; DeJarnette, E.; Zakrzewski, S. F. In *Chemistry and Biology of Pteridines*; Blair, J. A., Ed.; de Gruyter: Berlin, 1983; pp 293-297.

(13) Schwalbe, C. H.; Cody, V. In *Chemistry and Biology of Pteridines*; Blair, J. A., Ed.; de Gruyter: Berlin, 1983; pp 511-515.

(14) Cody, V.; Welsh, W. J.; Opitz, S.; Zakrzewski, S. F. In *QSAR in Design of Bioactive Compounds*; Kuchar, M., Ed.; J. R. Prous Science: Barcelona, Spain, 1984; pp 241-252.

Table V. Hydrogen Bonding

	D...A	D...A, Å	D-H, Å	H...A, Å	∠D-H...A, deg
DAHP					
N(2)-HA...N(3)		3.118	0.60	2.60	146
N(2)-HB...O(2')		3.063	0.52	2.66	137
N(4)-HA...O(2')		3.123	0.59	2.63	144
N(4)-HB...O(2*)		2.977	0.85	2.23	146
DAMP1					
N(2)-HA...Cl		3.19	0.95	2.32	153
N(2)-HB...Cl		3.19	0.83	2.38	163
N(4)-HA...N(3)		3.29	0.89	2.41	173
N(4)-HB...Cl		3.25	0.87	2.55	140
N(1)-H...Cl		3.23	0.79	2.53	151
DAMP2					
N(2)-HA...O(1)		2.90	0.86	2.00	176
N(2)-HB...O(2)		3.25	0.85	2.47	154
N(4)-HA...O(1)		2.93	0.89	2.19	141
N(4)-HB...N(3)		3.15	0.81	2.35	170
N(1)-H...O(3)		2.77	0.97	1.93	161
DAEP					
N(2)-HA...N(1)		3.11	0.92	2.25	155
N(2)-HB...N(3)		3.11	0.86	2.28	162
DAPP					
N(2)-HA...O(1)		2.98	0.89	2.16	153
N(2)-HB...O(3)		2.93	0.80	2.14	169
N(4)-HA...O(1)		2.97	0.85	2.19	154
N(4)-HB...N(3)		3.06			
N(1)-H...O(2)		2.76			

These data also show there is an enhancement in the changes in geometry upon N(1) protonation. For example, the bond angles involving N(3) and C(4) appear constant whereas those involving N(1), C(6), and C(5) show the effects of N(1) protonation; e.g., C(5)-C(6)-C(61) and C(6)-C(5)-C(7) are greater for protonated structures than the corresponding free base. The largest endocyclic bond angle changes are observed for C(2), N(1), and C(6) upon N(1) protonation.

The hydrogen bonding patterns in these structures (Table V) vary depending upon the solvents that are cocrystallized with the antifolates. In the case of DAEP free base, which crystallizes in a noncentrosymmetric space group, only the hydrogen atoms of N(2) are utilized to form pseudo base pair hydrogen bonds (N(2)...N(3); N(1)), similar to that observed in other antifolate structures.¹³ On the other hand, DAHP free base cocrystallizes with two molecules of dimethyl sulfoxide so that N(2) also forms an N...O hydrogen bond as well as the pseudo base pair. The protonated structures DAMP2 and DAPP are both ethane-sulfonate salts which form the same hydrogen bonding patterns involving N(2)...O bonds and N(4)...N(3) pseudo base pair hydrogen bonds. DAMP1 is a HCl salt which has an N(4)...N(3) pseudo base pair hydrogen bond and N...Cl hydrogen bonds.

Thus, analysis of these data show that for free base structures both N(2) and N(4) tend to form the same types of interactions: base pair dimerization involving both amine groups. When N(1) is protonated, N(2) tends to use both protons to hydrogen bond to the solvent oxygens or counterions, while N(4) maintains a preference to form the base pair dimer with one proton and to form another with a solvent oxygen.

Molecular Modeling. In order to assess the influence of ring substitution and N(1) protonation on pyrimidine structure, CNDO/2 (complete neglect of differential overlap) geometry-optimized molecular orbital calculations were carried out on these antifolates.¹⁴⁻¹⁶ These results showed the effects of N(1) protonation, of increased ring substitution, and of increased 6-alkyl substitution on the pyrimidine ring geometry. These data indicate that the major conformational effect of larger 6-alkyl substitutions is to increase the pyrimidine ring torsional distortions from pla-

(15) Welsh, W. J.; Cody, V.; Mark, J. E.; Zakrzewski, S. F. *Cancer Biochem. Biophys.* 1983, 7, 27-38.

(16) Welsh, W. J.; Mark, J. E.; Cody, V.; Zakrzewski, S. F. In *Chemistry and Biology of Pteridines*; Blair, J. A., Ed.; de Gruyter: Berlin, 1983; pp 463-468.

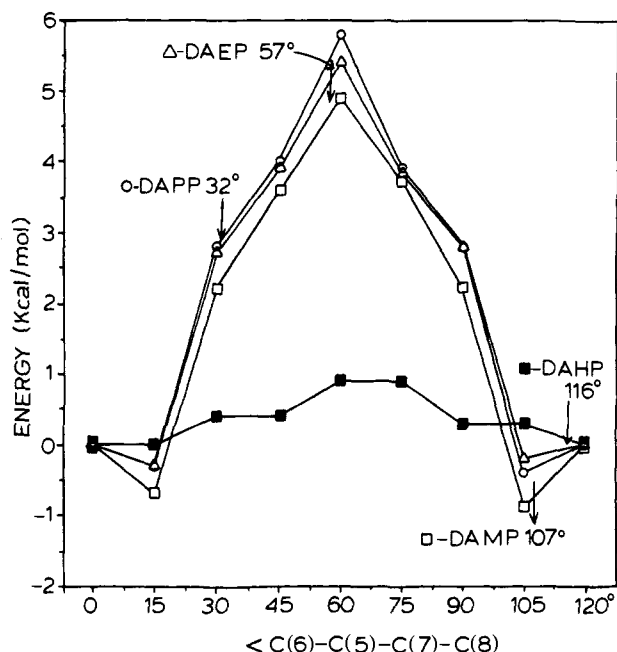


Figure 5. Geometry-optimized MM2P calculated conformational energy E vs. ϕ_{1-7} for DAHP, DAMP, DAEP, and DAPP, where energies are given relative to that calculated for $\phi = 0^\circ$ for each congener. The crystallographically observed conformations are also shown on the plot.

narity. There is also an increase in the C(6)–N(1) bond length and the C(6)–N(1)–C(2) angle. There appears to be little influence on these parameters from the addition of the 2,4-diamino groups of this ring system. In agreement with structural data, these results also showed that the pyrimidine ring distortions increase from the planarity observed in DAHP to a flattened boat for DAPP. While these CNDO/2 calculations have matched the patterns observed from the crystal structure data, the most serious discrepancies involved the 2,4-diamino geometry. Thus, molecular mechanics force field calculations using MM2P were carried out on this family of antifolates.

The full relaxation MM2P conformational energy profiles were determined for each of the structures considered here with respect to rotation ϕ_1 (C(6)–C(5)–C(7)–C(8)) of the adamantyl group about the C(5)–C(7) bond (Figure 5). For DAMP, DAEP, and DAPP the energy barriers to free rotation are large at ~ 6 kcal/mol, and all conformations in the range $30^\circ < \phi_1 < 90^\circ$ (within the 0–120° conformational space studied) are higher than 2 kcal/mol and thus energetically less accessible. In all three cases the maximum barrier is located at $\phi_1 = 60^\circ$, corresponding to a conformation in which the already existing steric conflicts between the adamantyl and C(6) substituent are further aggravated by steric interactions between the adamantyl group and the C(4) amino group. The E vs. ϕ_1 profile (Figure 5) for DAHP is by comparison quite flat due to the absence of a bulky 6-substituent giving rise to the severe steric interactions and concomitant high energy barriers associated with rotation of the adamantyl group. Since these energy barriers were computed with "full relaxation", these plots represent the path of least resistance along the potential energy surface.

A comparison of the crystallographic conformations for this series shows that both DAMP structures are low energy conformations, as is DAHP. However, the structure of DAEP is observed at the energy barrier near $\phi_1 = 60^\circ$. DAPP, an inactive antifolate in this series, is midway along the maximum energy profile at ~ 4 kcal/mol. Analysis of a second crystal structure form of DAEP¹² indicates that one of the two independent molecules in the lattice represents a high energy form and the other a minimum energy form. The adamantyl rings in this structure are rotationally disordered.

The contour plot (Figure 6) of the MM2P-calculated conformational energy E as a function of ϕ_1 and ϕ_2 (C(5)–C(6)–C(61)–C(61)) for DAEP illustrates the large fraction of confor-

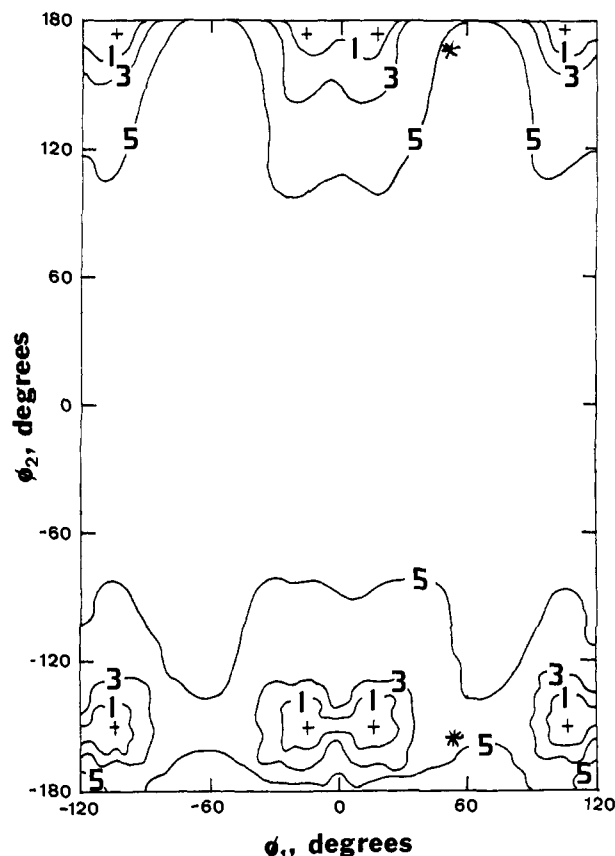


Figure 6. Geometry-optimized MM2P calculated conformational energy profile for the rotation about C(5)–C(7) and C(6)–C(61) of DAEP. The crystallographically observed conformations are indicated by * and the calculated energy minima by +.

mational domain space which is energetically prohibitive and, consequently, the high degree of conformational rigidity in these molecules. In fact, for some values of ϕ_1 , considerable ($\sim 15^\circ$) rotation of ϕ_2 (C(6)–C(61)) (Figure 6) does occur in a compensatory fashion to minimize the energy, but as is seen, no combination of ϕ_1 and ϕ_2 succeeds in reducing these energy barriers substantially. Also shown in this plot are the two disordered DAEP side-chain orientations which are in energetically unfavorable locations (Table II). The picture depicted here of energy minima separated by substantial energy barriers also points out the need for highly concerted motion among the substituents in moving from one energetically accessible conformation to another.

Other molecular mechanics calculations on DAMP identified energy minima at $\phi_1 = 0^\circ$ and 120° with domain sizes of roughly 10° .¹⁷ These data suggest that the location of energy minima at $\phi = 15^\circ$ (Figure 5) arises from the inclusion of molecular relaxation, which was not used in previous calculations.¹⁷ This methodological difference would also explain the smaller energy barriers found in the present calculations and the apparent absence of molecular distortions and consequent bowing in the other calculations.

Such conformational rigidity in the free (unbound) state may promote a favorable free energy of binding in that their binding to DHFR would not necessarily involve an appreciable loss in conformational versatility and hence in conformational entropy, as would be the case with a more flexible molecule such as MTX. This favorable (or more correctly less unfavorable) entropic contribution inherent in these constrained molecules may play an important and possibly dominant role¹⁸ in their potency. More specifically, DAEP may possess the optimal balance of lipo-

(17) Andrews, P. R.; Sadek, M.; Spark, M. J.; Winkler, D. A. *J. Med. Chem.* **1986**, *29*, 698–708.

(18) Dauber, P.; Osguthorpe, D. J.; Hagler, A. J. *Biochem. Soc. Trans.* **1982**, *10*, 312–313.

Table VI. Comparison of DAEP Pyrimidine Ring Geometry

	CNDO/2	MM2P	X-ray		CNDO/2	MM2P	X-ray
Bond Length, Å							
C(6)-N(1)	1.358	1.349	1.349	C(2)-N(2)	1.392	1.343	1.353
N(1)-C(2)	1.347	1.340	1.332	C(4)-N(4)	1.453	1.343	1.365
C(2)-N(3)	1.347	1.337	1.327	C(5)-C(7)	1.490	1.548	1.555
N(3)-C(4)	1.360	1.343	1.336	C(6)-C(61)	1.494	1.515	1.527
C(4)-C(5)	1.356	1.400	1.434				
C(5e)-C(6)	1.405	1.370	1.410				
RMSD	0.035	0.030			0.047	0.025	
Bond Angles, deg							
C(6)-N(1)-C(2)	116.9	119.5	117.0	N(1)-C(2)-N(2)	117.4	118.8	117.1
N(1)-C(2)-N(3)	125.2	122.3	125.1	N(3)-C(4)-N(4)	108.2	112.2	112.0
C(2)-N(3)-C(4)	114.4	117.2	117.2	C(4)-C(5)-C(7)	125.1	123.5	126.2
N(3)-C(4)-C(5)	125.5	122.8	123.7	C(5)-C(6)-C(61)	126.4	126.5	123.8
C(4)-C(5)-C(6)	110.9	111.4	111.9				
C(5)-C(6)-N(1)	123.5	121.8	123.5				
RMSD	1.4	1.4			1.9	1.8	
Torsion Angles, deg							
C(6)-N(1)-C(2)-N(3)	-9.1	-12.5	-9.1	N(3)-C(4)-C(5)-C(6)	-12.0	-13.6	-13.0
N(1)-C(2)-N(3)-C(4)	8.4	6.6	7.0	C(4)-C(5)-C(6)-N(1)	10.8	9.8	8.3
C(2)-N(3)-C(4)-C(5)	3.2	6.1	7.7	C(5)-C(6)-N(1)-C(2)	-1.7	2.7	2.7
RMSD	1.9	1.2		RMSD	1.9	1.2	

phlicity, steric specificity, and conformational rigidity to render it the most potent in this series (Table I). DAEP is unique among these congeners in that its structurally observed conformation corresponds to a high conformational energy state. This high energy conformation may be stabilized in the crystal by intermolecular interactions not considered in these force field calculations.

Of the four species considered in this study, it is noteworthy that DAHP and DAPP, the two least active, would also suffer the greatest loss in conformational entropy upon binding. Relative to DAEP, DAPP would lose an additional rotational degree of freedom associated with the terminal C-C bond of the propyl group and DAHP would lose at least some of the rotational flexibility of its adamantyl group. While clearly both reduced lipophilicity (in the case of DAHP) and steric limitations (in the case of DAPP) are other salient features used in rationalizing their decreased potency relative to DAMP and DAEP, the above point does emphasize the need to consider the entropic as well as the energetic and steric ramifications of drug binding.

This study shows that the most potent antifolate (i.e., DAEP) of this series of 6-substituted 5-adamantyl-diaminopyrimidines is observed in a high energy conformation and has disorder present in the ethyl side chain. This unusual stabilization may have ramifications with regard to its increased potency relative to the methyl and propyl analogues. Other data showing the interactions of these compounds in the active site of dihydrofolate reductase^{14,19} indicate that, at least on a qualitative level, the steric bulk of an added methyl group in the propyl analogue is not sufficient to explain its reduced activity.

Experimental Section

X-ray Crystal Structures. Intensity data for each structure determination were measured on a computer-controlled diffractometer using θ - 2θ scans. The structures were solved by using the direct methods program MULTAN²⁰ in conjunction with the NQEST²¹ figure of merit program. Refinement of the coordinates of all atoms, anisotropic thermal parameters of the non-hydrogens, and isotropic thermal parameters for the hydrogen atoms were obtained by using a full-matrix least-squares procedure that was based on F with weights based on $1/\sigma^2_F$. Differences in crystal quality account for the 2σ - 4σ variation in the cutoff value for "observed" reflections over background for these structures.

Crystal Data. 2,4-Diamino-5-(1-adamantyl)pyrimidine-Dimethyl Sulfoxide (DAHP): $C_{13}H_{20}H_4 \cdot C_2H_6SO$, $M_r = 400.61$, triclinic space

group $P-1$, $a = 11.013$ (1) Å, $b = 11.289$ (1) Å, $c = 9.992$ (1) Å, $\alpha = 95.9$ (1)°, $\beta = 109.8$ (1)°, $\gamma = 113.6$ (1)°, $Z = 2$, $d_c = 1.29$ g/cm³, $\mu = 24.5$ cm⁻¹, $\lambda = 1.5418$ Å (Cu K α), $R = 9.1\%$ for 3668 observations with $I > 3\sigma(I)$.

2,4-Diamino-5-(1-adamantyl)-6-methylpyrimidine Hydrochloride (DAMP1): $C_{15}H_{22}N_4Cl$, $M_r = 293.82$, monoclinic, $P2_1/n$, $a = 7.3256$ (6) Å, $b = 10.1752$ (9) Å, $c = 20.391$ (2) Å, $\beta = 99.505$ (9)°, $Z = 4$, $d_c = 1.30$ g/cm³, $\mu = 22.33$ cm⁻¹, $\lambda = 1.5418$ Å (Cu K α), $R = 5.0\%$ for 2366 observations with $I > 3\sigma(I)$.

2,4-Diamino-5-(1-adamantyl)-6-ethylpyrimidine (DAEP): $C_{16}H_{24}N_4$, $M_r = 273.40$, monoclinic, $P2_1$, $a = 13.2680$ (9) Å, $b = 7.0238$ (5) Å, $c = 7.7038$ (7) Å, $\beta = 93.815$ (2)°, $Z = 2$, $d_c = 1.27$ g/cm³, $\mu = 5.66$ cm⁻¹, $\lambda = 1.5418$ Å (Cu K α), $R = 6.2\%$ for 1277 observations with $I > 2\sigma(I)$.

2,4-Diamino-5-(1-adamantyl)-6-propylpyrimidinium Ethanesulfonate (DAPP): $C_{16}H_{27}N_4^{+} \cdot C_2H_5SO_3^{-}$, $M_r = C_{17}H_{22}N_4^{+} \cdot C_2H_5SO_3^{-}$, monoclinic, $P2_1/c$, $a = 6.761$ (2) Å, $b = 16.593$ (4) Å, $c = 18.032$ (4) Å, $\beta = 90.58$ (2)°, $Z = 4$, $d_c = 1.29$ g/cm³, $\mu = 16.05$ cm⁻¹, $\lambda = 1.5418$ Å (Cu K α), $R = 9.1\%$ for 2756 observations with $I > 4\sigma(I)$.

Calculated Structural Geometries. From an analysis of a set of structurally analogous lipophilic 2,4-diaminopyrimidines, MM2P force field parameters have been derived and tested.²² Results of the MM2P-calculated geometry for the diaminopyrimidine moiety in DAEP are summarized in Table VI along with the corresponding CNDO/2 calculated and X-ray observed values. In terms of RMSD (root-mean-square deviation) from the corresponding crystallographic values, the MM2P values are superior to the CNDO/2 values both overall and separately for bond lengths, bond angles, and torsion angles. Similar comparisons in the case of DAMP, DAPP, and DAHP corroborate these conclusions.

Potential energy calculations for the rotations about C(5)-C(7), C(6)-C(61), and C(61)-C(62) were done using the molecular mechanics program MM2P. The potential energies were calculated at 10° rotation steps of each bond, while holding the geometry fixed as observed in the crystal structure. The final energies were then adjusted so the minimum values were zero. Further refinement of the force field parameters were carried out as described.^{22,23}

Acknowledgment. This research was supported in part by research Grants NCI-34714 and FRA-187 (V.C.) American Cancer Society Faculty Research Award and by the Buffalo Foundation. We thank Sue Opitz and Dr. Sigmund Zakrzewski for providing samples of these antifolates.

Supplementary Material Available: Tables of atomic coordinates, equivalent isotropic thermal parameters, and hydrogen atom coordinates for the four adamantyl pyrimidine analogues (12 pages). Ordering information is given on any current masthead page.

(19) Cody, V. J. *Mol. Graphics* 1986, 4, 69-74.

(20) Germain, G.; Main, P.; Woolfson, M. M. *Acta Crystallogr., Sect. A: Cryst. Phys., Diffraction, Theor. Gen. Crystallogr.* 1971, 27, 368-376.

(21) DeTitta, G. T.; Edmonds, J. W.; Langs, D. A.; Hauptman, H. A. *Acta Crystallogr. Sect. A: Cryst. Phys., Diffraction, Theor. Gen. Crystallogr.* 1975, 31, 472-479.

(22) Welsh, W. J.; Cody, V. In *Chemistry and Biology of Pteridines 1986, Pteridines and Folic Acid Derivatives*; Cooper, B. A., Whitehead, V. M., Eds.; Walter de Gruyter: Berlin, 1986; pp 799-802.

(23) Welsh, W. J., submitted for publication in *J. Comput. Chem.*